Published in final edited form as:
Int J Radiat Oncol Biol Phys. 2007 October 1; 69(2): 589–597.

Whole Brain Radiation Therapy with Hippocampal Avoidance and Simultaneously Integrated Brain Metastases Boost: A Planning Study

Alonso N. Gutiérrez, Ph.D.[1], **David C. Westerly, M.Sc.**[1], **Wolfgang A. Tomé, Ph.D.**[1,2], **Hazim A. Jaradat, Ph.D.**[2], **Thomas R. Mackie, Ph.D.**[1,2,3], **Søren M. Bentzen, Ph.D., D.Sc.**[2], **Deepak Khuntia, M.D.**[2], and **Minesh P. Mehta, M.D.**[2]

1 *Department of Medical Physics, University of Wisconsin, School of Medicine and Public Health, Madison, WI, 53792, USA*

2 *Department of Human Oncology, University of Wisconsin, School of Medicine and Public Health, Madison, WI, 53792, USA*

3 *TomoTherapy, Inc., Madison, WI, 5717, USA*

Abstract

Purpose—To evaluate the feasibility of using tomotherapy to deliver whole brain radiotherapy (WBRT) with hippocampal avoidance, hypothesized to reduce the risk of memory function decline, and simultaneously integrated boost to brain metastases to improve intra-cranial tumor control.

Methods and Materials—Ten patients treated with radiosurgery and WBRT were replanned on tomotherapy using original CT scans and MR-CT fusion defined target and normal structure contours. The individually contoured hippocampus was used as dose-limiting structures (<6Gy); the whole brain dose was prescribed at 32.25 Gy to 95% in 15 fractions and simultaneous boost doses to individual brain metastases were 63 Gy to lesions ≥ 2.0cm in maximum diameter, and 70.8 Gy to lesions < 2.0cm. Plans were generated with a field width (FW) of 2.5cm, and in five patients with FW of 1.0cm. Plans were compared regarding conformation number (CN), prescription isodose to target volume (PITV) ratio, target coverage (TC), homogeneity index (HI), and mean normalized total dose (NTD_{mean}).

Results—A 1.0cm compared with 2.5cm FW significantly improved the dose distribution. Mean CN number improved from 0.55±0.16 to 0.60±0.13. Whole brain homogeneity improved by 32% (p<0.001). NTD_{mean} to the hippocampus were 5.9±1.3 and 5.8±1.9 Gy_2, for 2.5 and 1.0cm FW, respectively. Mean treatment delivery time for 2.5 and 1.0cm FW plans were 10.2±1.0 and 21.8±1.8 minutes.

Conclusions—Composite tomotherapy plans achieved 3 objectives: homogeneous whole brain dose distribution equivalent to conventional WBRT; conformal hippocampal avoidance; radiosurgically-equivalent dose distributions to individual metastases.

Address of Correspondence: Dr. Wolfgang A. Tomé, University of Wisconsin School of Medicine and Public Health, Department of Human Oncology, K4/344 Clinical Science Center, 600 Highland Ave., Madison, WI 53792, U.S.A, Tel: 001-608-263-8510, Fax: 001-608-263-9947, E-mail: tome@humonc.wisc.edu.

Conflict of Interest Notification:
T.R. M. has a financial interest in TomoTherapy, Inc., and therefore has a potential conflict of interest.

Keywords

tomotherapy; whole brain; brain metastases; conformal avoidance; hippocampus

I. Introduction

Whole brain radiation therapy (WBRT) is usually the primary treatment option for patients with multiple brain metastases extending median survival time approximately from 1 to 4 months. Survival has not been shown to increase in patients with multiple metastases with added stereotactic radiosurgery (SRS) (1) or radiosensitizers. (2) Different dose, timing, and fractionation schemas have been investigated but none have shown superior survival or neurologic improvement compared to standard schedules. (3,4) WBRT provides palliation of symptoms; the main treatment aim is prolongation of the time to neurocognitive decline and, related to this, maintaining the patient's quality of life (QOL) as long as possible. Radiation therapy is a mainstay in pursuing this aim, but may in itself also cause neurocognitive decline months after therapy. Long-term serious and permanent toxic effects including cognitive deterioration and cerebellar dysfunction have been described. (5) DeAngelis *et al.* suggests that as many as 11% of long term brain metastases survivors (>12 months) treated with WBRT develop dementia, especially with the use of larger dose-per-fraction schedules. (6)

A recent publication by our group presents a detailed analysis of the time course of neurocognitive function (NCF) decline in 8 prospectively measured domains in 208 brain metastases patients treated with 30 Gy WBRT. NCF, assessed by tests of memory, executive function, and fine motor coordination, were correlated to MRI-measured metastases volume regression. (7) NCF and survival were compared in 135 patients evaluable at 2 months with tumor shrinkage below (poor responders) and above (good responders) the population median. Mean NCF scores and brain metastases volume at 4 and 15 months were compared. Good responders experienced a significantly improved survival. For all tests, the median time to NCF deterioration was longer in good than in poor responders, with statistical significance seen for executive and fine motor function. However, memory functions were most susceptible to early decline, even in patients with non-progressing brain metastases. These findings suggest that achievement of macroscopic lesion control is an important treatment aim. Furthermore, strategies preserving memory-related NCF should be investigated.

Following WBRT, patients can present with progressively severe deficits in hippocampal-dependent functions. (8) Recent studies indicate that the functions of learning, memory (short and long term), and spatial information processing are affected by irradiation of the hippocampus; the current postulate is that although several functional areas of the brain are responsible for these functions, the stem cell compartment housing the necessary progenitor cells resides within the hippocampus and is exquisitely radiosensitive. Hence, irradiation of this compartment causes depletion of cells necessary for neurogenesis, especially for the memory domains. (9)

The above findings lead to the testable hypothesis that avoidance of the hippocampus during WBRT (WBRT-HA) may delay the onset and/or reduce the severity of neurocognitive deficits in survivors by selectively sparing stem cells responsible for post-WBRT neurogenesis. Further, the dose to clinically manifest brain metastases should be increased in an attempt to prolong the time to intracranial disease progression. However, the anatomical shape and central location of the hippocampus poses an interesting radiation delivery challenge. Kron *et al*. have shown that the large number of beam projections and helical delivery of tomotherapy permits good dose conformity to complex structures and superior conformal avoidance of critical structures indicating that tomotherapy may be of benefit for WBRT-HA. (10)

Proliferation of tumor cells during radiotherapy is an important postulated cause of treatment failure. (11) Studies have suggested that it is not necessarily just the high proliferation rate prior to initiation of radiotherapy, but rather the ability of the tumor to respond to cytotoxic trauma by accelerated repopulation. (12) Accelerated proliferation may be compensated for by an accelerated-boost, a concept well validated in trials of head-and-neck as well as non-small cell lung cancers. (13,14) Boosting of metastases has already been shown to improve local tumor control, and possibly survival, in patients with up to 10 lesions. (15) Bhatnagar *et al.* suggest a thought-provoking and challenging conclusion that radiosurgery may enhance survival in selected patients with multiple brain metastases. Helical tomotherapy has been previously shown to deliver comparable target coverage and conformity to brain lesions as standard radiotherapy techniques. (16–18) Additionally, delivery of boost dose to multiple metastases has been also been accomplished. (19)

In view of the above, we hypothesized that improved intracranial control of brain metastases could prolong the time to neurocognitive function decline. In order to achieve this goal, we would need to (1) conformally avoid the hippocampus, (2) treat the remaining whole brain to traditional WBRT-equivalent doses to sterilize micro-metastatic disease, and (3) simultaneously boost gross metastatic diseases to radiosurgical–equivalent doses. To meet these three objectives within a deliverable treatment plan, we investigated the unique delivery geometry of helical tomotherapy to generate a single, composite plan. This study additionally varied the pitch and field width to quantify its dosimetric impact on treatment plans in order to provide the physical treatment-planning and delivery mechanism that would allow us to test the hypothesis articulated above in a prospective clinical trial.

II. Methods and Materials

With approval by our Institutional Review Board, ten patients diagnosed with brain metastases and treated with linac-based SRS with or without WBRT in our institution were replanned with clinically deliverable helical tomotherapy. Seven of the ten patients had more than one brain metastasis. The number of metastases ranged from one to five with a mean of 2.5±1.4. Patient characteristics are shown in Table 1. The planning target volumes (PTV) for metastases ranged from 0.35 to 34.33 cm^3, median of 1.72 cm^3. Location of the metastases resembled previously published distribution results with the majority located in the cerebral hemispheres followed by the cerebellum. (20)

Patients were scanned by a computed tomography (CT) system (Discovery LS, GE Medical Systems, Milwaukee, WI) using axial scan mode. CT scan implemented 1.25 mm slice thickness over the entire head region. Each patient also underwent a T1-weighted, 3-D Spoiled Gradient (SPGR), post-contrast axial magnetic resonance imaging (MRI) scan using a 1.5T MR scanner (GE Medical Systems, Milwaukee, WI) with 1.25mm slice thickness. Anatomical contours were delineated on the fused CT and MR image sets in the treatment planning system (TPS) Pinnacle$^{3®}$ Ver.8.1s (Philips Medical System, Fitchburg WI), Figure 1. The hippocampus was manually contoured while the whole brain and eyes were contoured using model-based segmentation. A 2 mm volumetric margin expansion was applied to the visible metastases to create the PTV based on the interfractional image registration accuracy of helical tomotherapy. (21). A 5 mm volumetric margin expansion was applied to the hippocampus. A whole brain clinical target volume (WB-CTV) was generated by subtracting the PTV metastasis volumes and the hippocampus with the 5 mm expansion volume from the whole brain contour. CT images and associated contours were transferred to tomotherapy TPS (TomoTherapy Inc, Madison, WI) from Pinnacle$^{3®}$ TPS via DICOM-RT protocol.

Helical tomotherapy allows the delivery of image-guided, intensity-modulated radiation therapy (IG-IMRT). (22) Details of the inverse planning algorithm used in tomotherapy have

been previously described. (23) Tomotherapy optimization is guided using several parameters unique to helical tomotherapy. The user defines the prescription to the tumor structures, field width defined by the primary jaws, modulation factor (MF), pitch, and resolution of calculated dose grid. In tomotherapy, the field width is defined as the slice thickness of the radiation field projected at the isocenter along the gantry rotation axis. Current Hi-ART® machines typically have three commissioned field widths of approximately 1.0, 2.5, and 5.0cm. The modulation factor is defined as the ratio of the maximum leaf opening time to the average opening time of all of the non-zero leaf opening times. The pitch is defined as the ratio of the distance the couch travels per rotation to the field width at the gantry axis.

For this study, the majority of plans were generated using a 2.5cm FW to obtain the most conformal treatment plan deliverable in a reasonable time period. Selected patients were also planned with a nominal 1.0cm FW. Pitches equivalent to 0.866 divided by an integer were used in this study based on the thread effect work by Kissick *et al*. (24). For all plans, the modulation factor was set to 3.5. In general, a higher modulation factor facilitates higher dose gradients; however, the benefit of increasing the modulation factor quickly diminishes above 3.0. Higher modulation factors lead to longer treatment times. Prescription doses were 32.25 Gy to 95% volume of the whole brain (WB-CTV), 63 Gy to 95% volume of metastases ≥2.0cm in maximum diameter, and 70.8 Gy to 95% volume of metastases <2.0cm in 15 treatment fractions. These dose fractionation schedules were derived from RTOG 0023 such that the expected acute complications, NTD_{10}, were matched for the target volumes treated to the boost dose in RTOG 0023. (25) Directional blocking was utilized for the eyes, and the dose constraint applied was no more than 50% of the eyes receive more than 5Gy. Maximum dose constraints to the eyes and hippocampus were 5 and 6Gy, respectively. If a brain metastasis was in close proximity to the chiasm, maximum dose to the chiasm was constrained to 55Gy. Since the brain stem was part of the whole brain CTV, it was assigned the same dose constraints as the WB-CTV.

During the planning process, tomotherapy TPS downsampled CT image resolution to 128 × 128 pixels in each slice and increased slice width from 1.25mm to 2.5mm over the entire CT image volume set. This was necessary to reduce the amount of memory required for optimization. In addition, patient-specific quality assurance was performed for a 1.0cm treatment plan to test delivery feasibility. A 1.0cm field width test case was selected as this would represent a “worse case” delivery situations due to longer treatment time and higher modulation factor.

Plan comparison criteria

Treatment plan comparison metrics compared the following criteria: conformation number (CN), prescription isodose to target volume (PITV) ratio, target coverage (TC), homogeneity index (HI), and mean normalized total dose (NTD_{mean}) for critical structures. The PTV of the metastases was used as the target volume.

Dose conformity was characterized by the conformation number (CN) as proposed by van’t Riet *et al.*, which accounts for dose coverage and normal tissue irradiation to prescription dose. (26) The CN is defined as:

$$CN = \frac{V_{T,pres}}{V_T} \cdot \frac{V_{T,pres}}{V_{pres}} = \frac{V_{T,pres}^2}{V_T \cdot V_{pres}} \quad (1)$$

where V_{pres} is the volume receiving a dose greater than or equal to the prescription dose, $V_{T,pres}$ is the volume within the target receiving a dose equal to or greater than the prescription dose, and V_T is the planning target volume. The first term in Equation 1 depicts the target coverage. The second factor represents the proportion of V_{pres} that actually covers the target

volume. The conformation number ranges between 0 and 1. A value of 1 represents a prescription isodose covering the target volume exactly without irradiating normal tissue and indicates optimal conformation.

For comparison and reference purposes, the prescription isodose to target volume ratio and the target coverage were computed. The prescription isodose volume to target volume ratio (PITV) is defined as follows: (27)

$$PITV = \frac{V_{pres}}{V_T} \tag{2}$$

PITV values < 1.0 indicate that the target volume is not completely covered by the prescription isodose volume, whereas values > 1.0 indicated a too liberal coverage. Note, that PITV ratios near 1.0 do not imply that the two volumes closely coincide spatially unless the PTV is completely contained within the prescription isodose volume. The target coverage (TC) parameter describes the fraction of the target volume receiving at least the prescription dose and is defined as:

$$TC = \frac{V_{T,pres}}{V_T} \tag{3}$$

For perfect coverage, TC equals 1.0.

Dose homogeneity in the target volumes were quantified by the homogeneity index (HI) as recommended by the ICRU. (28) The HI is defined as the highest dose delivered to 2% of the target volume ($D_{2\%}$) minus the dose delivered to 98% of the target volume ($D_{98\%}$) divided by the median dose (D_{median}) of the target volume.

$$HI = \frac{D_{2\%} - D_{98\%}}{D_{median}} \tag{4}$$

Smaller values of HI correspond to more homogenous irradiation of the target volume. A value of 0 corresponds to absolute homogeneity of dose within the target.

Normal tissue sparing was quantified using maximum and mean normalized total dose (NTD). (29) NTD is defined as the total dose, if delivered in 2 Gy fractions, that would have the same biological effect as the actual treatment fractionation schedule for a specific tissue. An α/β ratio of 2 Gy was assumed for the hippocampus, and a ratio of 3 Gy for the eyes.

III. Results

Metastases Analysis

Table 2 lists the mean indices values for all metastases as a function of field width and pitch for tomotherapy plans. Mean CN values showed a 9% improvement ($p < 0.011$) when reducing the FW from 2.5 to 1.0cm. Mean PITV values (± 1 SD) for metastases using a 2.5cm FW showed little dependence on pitch but improved significantly by 15% ($p < 0.038$) when decreasing the FW from 2.5 to 1.0cm. There was no significant difference in mean TC values among the pitches with 2.5cm FW and between the two field widths. Additionally, mean HI values were invariant with pitch using the larger FW however showed a significant 13% ($p < 0.011$) improvement with a smaller FW.

Previous studies found that dose conformity of gamma knife radiosurgery plans improved with increasing PTV volume. (30) To test whether this was the case for tomotherapy plans, metastases were sorted into two volume bins, using a cut point of 2.05 cm^3. Table 3 shows

mean and standard deviation of the dosimetric indices for 2.5cm FW plans. The mean CN values were 60% higher (0.444 vs. 0.708) for volumes greater than 2.05 cm^3. Similarly, mean PITV value were 43% lower ($p < 0.0003$) for volumes greater than 2.05 cm^3. Homogeneity also improved by 14% ($p < 0.049$) for larger volumes. Target coverage was slightly higher for smaller volume metastases. No significant impact of lesion volume was assessed with the 1.0cm FW due to the insufficient number of metastases in each dose bin.

Whole Brain Analysis

Table 2 lists the mean index values of dose coverage for the whole brain. No significant difference was noted among the pitches using the 2.5cm FW; however, a 32% ($p < 0.001$) reduction of mean HI value was noted between the 2.5 and 1.0cm FW. The improved homogeneity with the smaller field width was also visually notable in the relative, cumulative dose volume histograms (DVH) during optimization—see Figure 2. Mean TC values are also shown in Table 2. For various pitches and field widths, differences in mean TC values were not significant and all showed adequate whole brain coverage.

Hippocampus Dose

Our main planning objective was to reduce the dose to the hippocampus as much as possible without jeopardizing coverage of the metastases and whole brain. Table 4 lists the dose statistics for the hippocampus of each patient as a function of pitch and field width. For the majority of patients, the mean dose was approximately 6.0 Gy_2 with the exception of patient 9 who had 5 metastases. The larger mean dose to the hippocampus for this patient can be attributed to the fact that 3 of the 5 metastases were in the same delivery plane as the hippocampus and eyes—slightly limiting conformal avoidance ability by reducing the number of delivery projections. No significant difference in average NTD_{mean} to the hippocampus was observed among the pitches using the 2.5cm FW and between the 1.0 and 2.5cm FW. In terms of maximum dose, there was no difference in the average maximum NTD to the hippocampus among the pitches using the 2.5cm FW. A 13% (16.9 vs. 14.7, $p < 0.02$) average maximum NTD reduction was noted when the FW was reduced from 2.5 to 1.0cm.

Eye Dose and Treatment parameters

Table 5 shows the average NTD_{mean} to the eyes as a function of pitch and field width. Average NTD_{mean} to the eyes did not differ significantly among pitches using a 2.5cm FW. A 19% reduction ($p < 0.06$) in average NTD_{mean} was noted when reducing the FW to 1.0cm. Mean modulation factor (MF) for treatment plans increased as the pitch increased for a fixed FW. Reduction of the FW to 1.0cm resulted in a mean modulation factor increase of 13% ($p < 0.0008$). The increase in the mean modulation factor for the smaller FW may be attributed to the decrease in the mean leaf open time. For a fixed pitch, open time per gantry rotation for a given leaf required to fully irradiate a fixed target decreases as the FW decreases since additional gantry rotations can be used to make up for the decreased leaf open times in a given rotation.

Mean treatment plan parameter values for gantry period and treatment time are also shown in Table 5. For 2.5cm FW, gantry period increased as pitch increased. More specifically, the percent increase in pitch is almost numerically equivalent to the percent increase in gantry period. A 34% increase of pitch from 0.215 to 0.289 leads to a 36% increase of mean gantry period from 19.0 to 25.9 seconds. Similarly, a 50% increase from 0.289 to 0.433 produced a 48% increase of the mean gantry period from 25.9 to 38.3 seconds. This effect can be attributed to the fact that the total amount of energy deposited in the patient must be independent of pitch—assuming a constant dose prescription. Since the dose rate is fixed, the gantry rotation speed decreases—increasing the gantry period and decreasing the number of rotations—to compensate for the decreased time that is spent irradiating the fixed volume. The observation

that pitch is proportional to gantry period agrees with the work on modeling simple tomotherapy dose distributions performed by Fenwick *et. al.* (31) Mean treatment times did not vary among pitches with the 2.5cm FW. The overall treatment time for the pitches with the 2.5cm FW was roughly 10 minutes of beam on time. With 1.0cm FW, mean treatment time increased 126% ($p < 0.0001$) from 10.2 to 21.8 minutes.

Patient-specific delivery quality assurance was performed for one treatment plan using a 1.0cm FW to verify delivery feasibility. The treatment plan was delivered in the tomotherapy cylindrical solid water phantom. Dose measured using both KODAK EDR2® ready pack film (Eastman Kodak Company, Rochester NY) and an A1SL Exradin ion chamber (Standard Imaging, Middleton, WI) shows excellent correlation between calculated and delivered dose distributions—Figure 3. Figure 3a shows two profiles in the coronal plane: one across the metastasis and another across the hippocampus. Figure 3b shows the results of a gamma index distribution map (acceptance criterion: 3% or 3mm DTA) as described by Low *et. al*. (32) Values of the gamma index larger than 1 correspond to locations where the calculation does not meet the acceptance criterion.

IV. Discussion

In this study, a composite helical tomotherapy plan was constructed to meet three particular objectives: (1) deliver radiosurgical-equivalent dose distributions to multiple metastases, (2) deliver a homogeneous dose distribution to the whole brain, equivalent to conventional WBRT, and (3) conformally avoid the hippocampus without jeopardizing whole brain or metastases coverage. To judge the usefulness of this composite technique, the quality of each component must exceed or match the current accepted standard of care. For metastases, a measure of the quality of the dose distribution can be assessed through indices such as conformity. For the whole brain, the assessment can be made by target coverage and homogeneity. For the conformal avoidance of the hippocampus, the dose should be reduced as much as possible with sharp dose gradient fall off.

To assess the quality of our plans, we compared our results with previous studies on radiosurgery. Nakamura *et al.* compiled dose conformity statistics on 1338 lesions treated with gamma knife radiosurgery and reported measures of conformity equivalent to our CN and PITV. (30) It is important to mention that the CN value is a better quality measure than the PITV ratio, for it accounts for spatial deviations as well as conformity between the prescription isodose and target volume. Nakamura *et al*. found a median CN value of 0.56 for all lesions as our study found a median value of 0.59. For reference purposes, we also compared our median values of PITV for the different volume quartiles quoted. They found for the second target volume (0.25 –1.5 cm^3), third target volume (1.6–5.5 cm^3), and fourth target volume (5.6–55.9 cm^3) quartile median CI values of 1.85, 1.53, and 1.35, respectively. For our plans, using the same target volume bins, median values of 2.22, 1.34, and 1.17, respectively, were obtained. Thus, it appears our technique is capable of producing similar or better conformity than gamma knife radiosurgery for target volumes greater than 1.5 cm^3.

For volumes less than 1.5 cm^3, we found the size of the longitudinal dimension of the target volume relative to the FW becomes significant. If the FW is much larger, a “ballooning” of the isodose line in the longitudinal direction occurs thus generating a larger prescription dose volume yielding an increased PITV ratio. This was evident when one observes the median PITV values of the second target volume quartile as a function of FW. Median PITV values for 2.5 and 1.0cm FW were 2.25 and 1.74, respectively. Hence, it appears that for lesions smaller than 1.5 cm^3 it would be beneficial to use a smaller FW to reduce the volume of normal tissue irradiated to prescription dose. Similarly, Nakamura *et al.* noted worse conformity for smaller target volumes; however, no complications of radiosurgery were observed. They

concluded that conformity, due to its relative and not absolute nature, does not seem to be very important for very small, absolute volume lesions (< 1.0 cm^3). Our results indicate that this technique is capable of delivering radiosurgical quality dose distributions to multiple metastases of varying size even when used in combination with WBRT-HA.

As for the WBRT component, adequate target coverage is achieved as shown by the mean TC values in Table 2. In terms of homogeneity, the HI improves significantly when using a 1.0cm FW. Traditionally, WBRT without hippocampal avoidance is delivered with two lateral-opposed beams producing inhomogeneities on the order of 6–8%. From Table 2, we note that the inhomogeneity is on the order of 48% for tomotherapy plans. However, the values quoted in the table are meant to be interpreted relatively and not absolutely. Since the hippocampus and metastases are both located within the brain, two opposite objectives are being accomplished. Even though the hippocampus and metastases are not considered part of the brain structure, their respective dose gradients fall within the brain structure. Therefore, the numerator in Equation 4 governing the HI value is purposely increased leading to larger HI values. Hence, absolute values of HI indexes obtained when concomitantly conformally avoiding and selectively boosting are not a good measure of the true homogeneity of the entire brain. A better index of true overall homogeneity could be the measure of the full width half maximum (FWHM) of the differential DVH—since the tails would be excluded. Nonetheless, excluding the artificial low and high dose tails on the DVH, the majority of the whole brain dose is quite homogeneous as would be seen with traditional irradiation techniques.

Conformal avoidance of the hippocampus during WBRT to preserve neurocognitive function is a novel idea. (33) As previously mentioned, recent studies suggest that the pathogenesis of radiation induced neurocognitive deficit may—at least in part—be due to radiation injury to proliferating neuronal progenitor cells in the sub granular zone of the hippocampus. We are cognizant that several other regions of the brain are involved in memory processing and retention functions, and emphasize that this specific testable hypothesis focuses on sparing the migrating stem cell compartment in the hippocampus responsible for post-WBRT neurogenesis as a component of preserving memory function. This does not implicate structural damage to a specific brain location. The novelty of hippocampal avoidance to delay the onset of neurocognitive deficits poses many unanswered questions. What is the dose threshold below which hippocampal stem cell neurogenesis is preserved to a clinically relevant extent? In our plans, the lowest average NTD_{mean} to the hippocampus achievable was 0.39 Gy_2 per fraction (5.8 Gy_2 total dose) using the 1.0cm FW. Is this dose low enough to not affect memory-related NCF in humans? The answer remains uncertain until WBRT-HA is implemented clinically.

Another potential concern is whether hippocampal avoidance leads to loss of tumor control for metastases found in or close to this region. A study carried out in our institution evaluated MR scans of 100 patients with brain metastases (n = 272), specifically in terms of distribution, and identified that only 9 (3.3%) were within 5mm of the hippocampus, implying that a 5mm margin around the hippocampus for conformal avoidance would be unlikely to result in an inordinately high failure rate. (34) Moreover, for patients presenting with a metastasis in close proximity to the hippocampus, it may be possible to sacrifice portions of the hippocampus (or ipsilateral hippocampus entirely) adjacent to the metastasis while still avoiding the contralateral portion.

This integrated technique of hippocampal avoidance, WBRT, and integrated boosts to multiple metastases delivered with a single helical tomotherapy plan seems to match the accepted quality of each independent component. While the 1.0cm FW improved the mean index values of PITV, CN, and HI for the metastases, homogeneity of the whole brain dose, and reduced the mean dose to the eyes, the treatment time more than doubled relative to that of a 2.5cm FW. To take advantage of the benefits from a smaller FW on the metastases while maintaining an

overall fast treatment time, two treatment plans could be generated and delivered sequentially. The treatment planning for both of these would have to be done together so that the effect of the 2.5cm FW could be included in the 1.0cm FW plan. The treatment plan with a 2.5cm FW setting would deliver the whole brain dose with hippocampus avoidance then the 1.0cm FW could be delivered targeting only the multiple metastases. Furthermore, the notion of dynamically modulating the FW during treatment would in theory increase conformity to metastases of varying volumes, improve homogeneity to the whole brain, and reduce dose to the hippocampus in the optimal treatment delivery time. (35)

V. Conclusion

We investigated the use of helical tomotherapy for the delivery of WBRT with hippocampal avoidance (WBRT-HA) and simultaneously integrated multiple metastases boost. We performed dosimetric comparisons among treatment plans as a function of pitch and field width. It was noted that the smaller field width (1.0cm) improved the mean index values of PITV, CN, and HI for metastases, dose homogeneity to the whole brain, and reduced the mean dose to the eyes. Average NTD_{mean} to the hippocampus remained invariant among different pitches and field widths studied. Treatment times were more than doubled using the 1.0 compared with the 2.5cm FW. Patient-specific delivery quality assurance performed in a cylindrical solid water phantom verified feasibility of treatment plan delivery. The ability to deliver radiosurgical quality dose distributions to multiple metastases, a homogeneous dose distribution to the whole brain, and conformally avoid the hippocampus in a single treatment plan is unique to helical tomotherapy.

Acknowledgements

Authors gratefully acknowledge support of NIH National Cancer Institute Grant 5 T32 GM08349, 5 RO1 CA109656, and P01 CA088960.

References

1. Andrew DW, Scott CB, Sperduto PW, et al. Whole brain radiation therapy with or without stereotactic radiosurgery boost for patients with one to three brain metastases: Phase III results of the RTOG 9508 randomised trial. Lancet 2004;363:1665–72. [PubMed: 15158627]
2. Shaw E, Scott C, Suh J, et al. RSRS13 plus cranial radiation therapy in patients with brain metastases: Comparison with the Radiation Therapy Oncology Group Recursive Partitioning Analysis Brain Metastases Database. J Clin Oncol 2003;21:2364–71. [PubMed: 12805339]
3. Tsao MN, Lloyd NS, Wong RKS, et al. Radiotherapeutic Management of Brain Metastasis: A Systemic Review and Meta-Analysis. Cancer Treatment Reviews 2005;31:256–273. [PubMed: 15951117]
4. Mehta MP, Tsao MN, Whelan TJ, et al. The American Society for Therapeutic Radiology and Oncology (ASTRO) Evidence Based Review of the Role of Radiosurgery for Brain Metastasis. Int J Radiat Oncol Biol Phys 2005;63(1):37–46. [PubMed: 16111570]
5. Roman DD, Sperduto PW. Neuropsychological effects of cranial radiation: Current knowledge and future directions. Int J Radiat Oncol Biol Phys 1995;31:983–998. [PubMed: 7860415]
6. DeAngelis LM, Delattre JY, Posner JB. Radiation-induced dementia in patients cured of brain metastases. Neurology 1989;39:789–796. [PubMed: 2725874]
7. Li J, Bentzen SM, Renschler M, et al. Regression After Whole-Brain Radiation Therapy for Brain Metastases Correlates with Survival and Improved Neurocognitive Function. J Clin Oncol 2007;25 (10):1260–6. [PubMed: 17401015]
8. Abayomi OK. Pathogenesis of irradiation-induced cognitive dysfunction. Acta Oncol 1996;35:659–663. [PubMed: 8938210]
9. Monje ML, Mizumatsu S, Fike JR. Irradiation induces neural precursor-cell dysfunction. Nature Medicine 2002;8:955–962.

10. Kron T, Chen J, Grant D, et al. Lung sparing in chest wall radiotherapy using 3D conformal RT, IMRT, IMAT, and helical tomotherapy: a planning comparison. Radiotherapy Oncol 2002;65:S17–S18.
11. Kim JJ, Tannock IF. Repopulation of cancer cells during therapy: an important cause of treatment failure. Nat Rev Cancer 2005;5(7):516–25. [PubMed: 15965493]
12. Wilson GD, Saunders MI, Dische S, et al. Pre-treatment proliferation and the outcome of conventional and accelerated radiotherapy. Eur J Cancer 2006;42(3):363–71. [PubMed: 16386890]
13. Dische S, Saunders MI. The CHART regimen and morbidity. Acta Oncol 1999;38(2):147–52. [PubMed: 10227434]
14. Belani CP, Wang W, Johnson DH, et al. Phase III Study of the Eastern Cooperative Oncology Group (ECOG 2597): Induction Chemotherapy Followed by Either Standard Thoracic Radiotherapy or Hyperfractionated Accelerated Radiotherapy for Patients with Unresectable Stage IIIA & B Non-Small Cell Lung Cancer. J Clin Oncol 2005;23(16):3753–3760.
15. Bhatnagar AK, Flickinger JC, Kondziolka D, et al. Stereotactic radiosurgery for four or more intracranial metastases. Int J Radiat Oncol Biol Phys 2006;64:893–903.
16. Cozzi L, Clivio A, Bauman G, et al. Comparison of advanced irradiation techniques with photons for benign intracranial tumours. Rad Oncol 2006;80:268–273.
17. Penagaricano JA, Yan Y, Shi C, et al. Dosimetric comparison of Helical Tomotherapy and Gamma Knife Stereotactic Radiosurgery for single brain metastasis. Rad Oncol 2006;26(1)
18. Soisson ET, Tomé WA, Richards GM, et al. Comparison of linac based fractionated stereotactic radiotherapy and tomotherapy treatment plans for skull-base tumors. Rad Oncol 2005;78:313–321.
19. Bauman G, Yartsev S, Fisher B, et al. Simultaneous Infield Boost With Helical Tomotherapy for Patients With 1 to 3 Brain Metastases. Am J Clin Oncol 2007;30(1):38–44. [PubMed: 17278893]
20. Delattre JY, Krol G, Thaler HT, et al. Distribution of brain metastases. Arch Neurol 1988;45:741–744. [PubMed: 3390029]
21. Boswell S, Tomé WA, Jeraj R, et al. Automatic registration of megavoltage to kilovoltage CT images in helical tomotherapy: An evaluation of the setup verification process for the special case of a rigid head phantom. Med Phys 2006;33(11):4395–4404. [PubMed: 17153418]
22. Mackie TR, Balog J, Swerdloff S, et al. Tomotherapy: a new concept for the delivery of conformal radiotherapy. Med Phys 1993;20:1709–19. [PubMed: 8309444]
23. Shepard DM, Olivera GH, Reckwerdt PJ, et al. Iterative approaches to dose optimization in tomotherapy. Phys Med Biol 2000;45:69–90. [PubMed: 10661584]
24. Kissick MW, Fenwick J, James JA, et al. The helical tomotherapy thread effect. Med Phys 2005;32:1414–23. [PubMed: 15984692]
25. Cardinale R, Won M, Choucair A, et al. A phase II trial of accelerated radiotherapy using weekly stereotactic conformal boost for supratentorial glioblastoma multiforme: RTOG 0023. Int J Radiat Oncol Biol Phys 2006;65(5):1422–8. [PubMed: 16750317]
26. van't Riet A, Mak AC, Moerland MA. A conformation number to quantify the degree of conformality in brachytherapy and external beam irradiation: Application to the prostate. Int J Radiat Oncol Biol Phys 1997;37:731–736. [PubMed: 9112473]
27. Shaw E, Kline R, Gillin M, et al. Radiation Therapy Oncology Group: radiosurgery quality assurance guidelines. Int J Radiat Oncol Biol Phys 1993;27:1231–9. [PubMed: 8262852]
28. Prescribing, Recording, and Reporting Photon Beam Therapy, International Commission on radiation Units and measurements, ICRU Report 62.
29. Lebesque JV, Keus RB. The simultaneous boost technique: the concept of relative normalized total dose. Radiother Oncol 1991;22:45–55. [PubMed: 1947212]
30. Nakamura JL, Verhey LJ, Smith V, et al. Dose conformity of gamma knife radiosurgery and risk factors for complications. Int J Radiat Oncol Biol Phys 2001;51:1313–1319. [PubMed: 11728692]
31. Fenwick JD, Tomé WA, Kissick MW, et al. Modelling simple helically delivered dose distributions. Phys Med Biol 2005;50:1505–17. [PubMed: 15798340]
32. Low DA, Harms WB, Mutic S, et al. A technique for the quantitative evaluation of dose distributions. Med Phys 1998;25(5):656–661. [PubMed: 9608475]

33. Khuntia D, Brown P, Li J, et al. Whole-brain radiotherapy in the management of brain metastasis. J Clin Oncol 2006;24:1295–1304. [PubMed: 16525185]

34. Ghia A, Tomé WA, Thomas S, et al. Distribution of Brain Metastases in Relation to the Hippocampus: Implications for Neurocognitive Functional Preservation. Int J Radiat Onc Bio Phys. 2007In Press

35. Yang JN, Mackie TR, Reckwerdt P. An investigation of tomotherapy beam delivery. Med Phys 1997;24(3):425–36. [PubMed: 9089594]

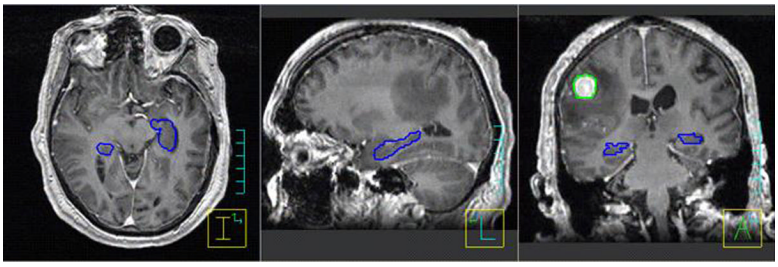

Figure 1.
Example segmentation of single brain metastasis (*green*) and hippocampus (*blue*) in a T1-weighted 3D-SPGR MR image data set of 1.25 mm slice thickness.

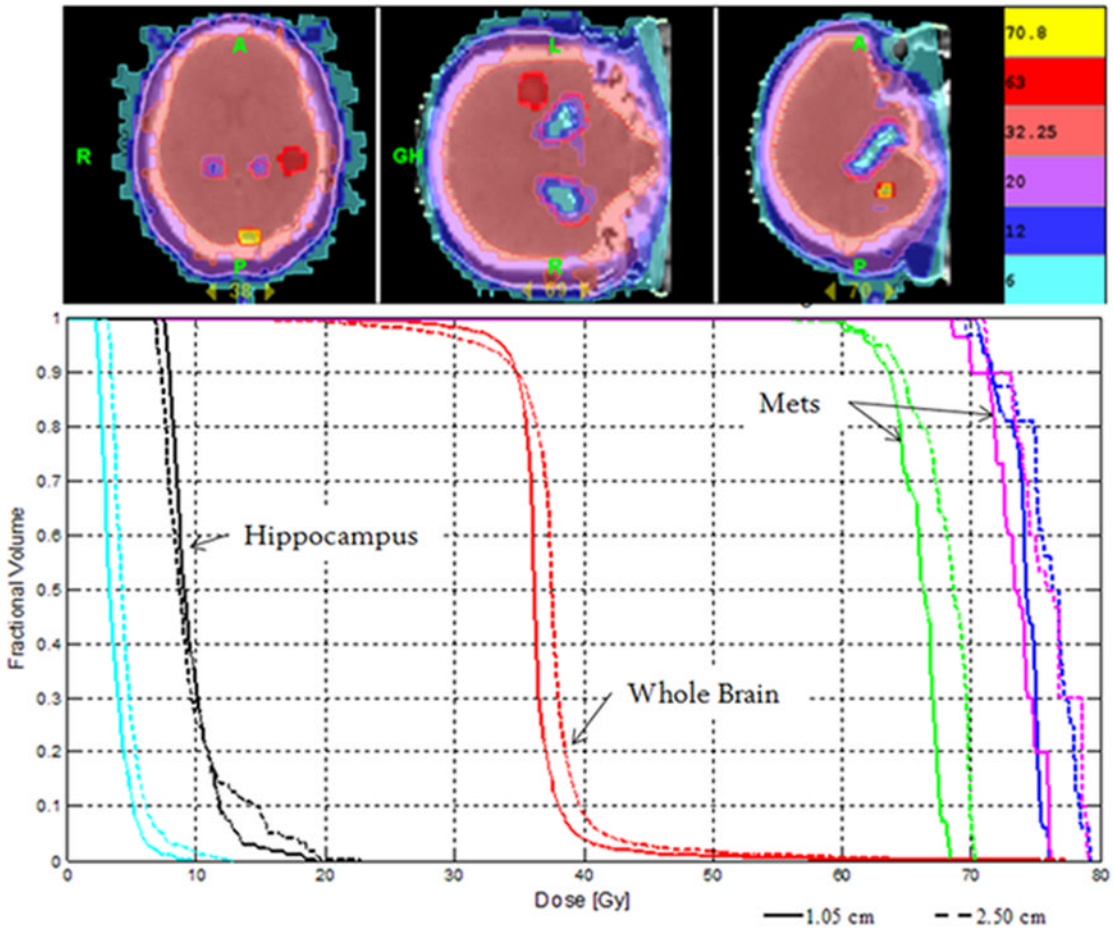

Figure 2.

(**Top**) Example isodose distribution of WBRT-HA with SIB of three metastases using helical tomotherapy. (**Bottom**) Corresponding cumulative, normalized DVH for WBRT-HA with SIB to three metastases. Two metastases prescribed to 70.8 Gy (*magenta* & *blue*), one metastasis to 63 Gy (*green*), whole brain (*red*) to 32.25 Gy. Hippocampus (*black*) and eyes (*cyan*) are shown. Dashed line represents plan with 1.0cm FW, and solid line represents plan with 2.5cm FW—both pitch of 0.289. *Plans normalized to prescription dose for comparison purposes.*

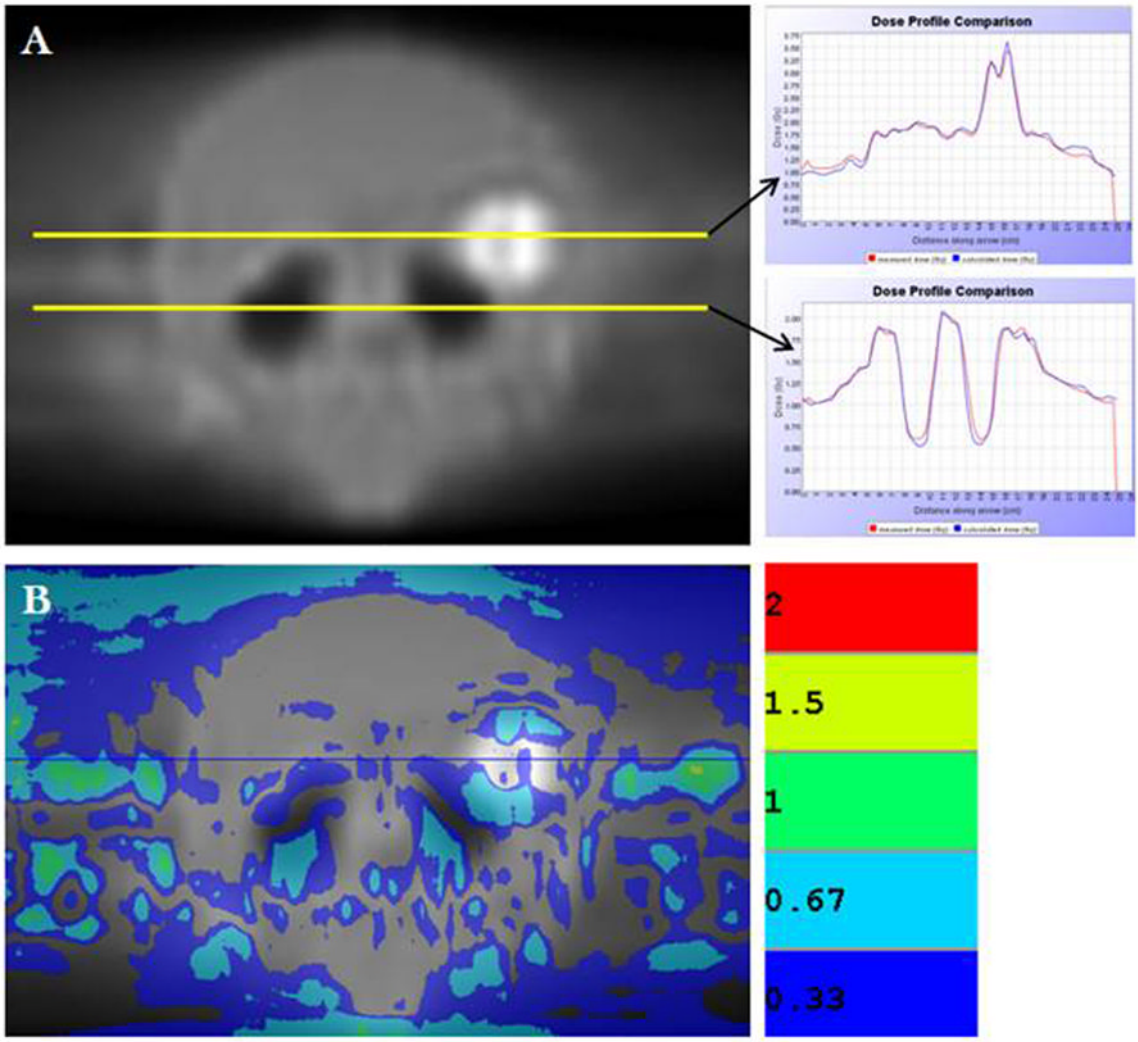

Figure 3.

(**A**) EDR2® film of coronal plane for sample patient treatment plan delivered in tomotherapy cylindrical solid water phantom. Profiles were acquired through metastasis (*top yellow line*) and hippocampus (*bottom yellow line*). Both profiles show superior correlation between measured and calculated dose distributions. (**B**) Gamma index distribution map between calculated and measured planar dose distributions shows good correlation.

Table 1

Metastases Description and Treatment Plan Prescriptions

Patient no.	Metastases	PTV Volume (cc)	Prescription Dose (Gy)
1	3	1.27	70.8
		4.35	63.0
		0.59	70.8
2	4	34.33	63.0
		17.99	63.0
		5.24	63.0
		1.20	70.8
3	4	0.90	70.8
		0.67	70.8
		0.51	70.8
		0.35	70.8
4	2	3.30	70.8
		3.57	70.8
5	2	0.51	70.8
		0.51	70.8
6	1	3.34	63.0
7	1	0.87	70.8
8	2	9.15	63.0
		2.05	70.8
9	5	6.24	63.0
		2.01	70.8
		1.62	70.8
		0.79	70.8
		1.72	70.8
10	1	2.63	70.8
Mean	2.5 ± 1.4	4.2 ± 7.3	

Abbreviations: PTV = planning target volume

Table 2

Statistical Analysis of Indices for Metastases and Whole Brain in Tomotherapy Plans as Functions of Field Width (FW) and Pitch.

	Mean and standard deviation				*p* value	
	2.5 cm FW			1.0 cm FW	0.215 vs. 0.433	$0.289_{2.5}$ vs. $0.289_{1.0}$
Index	**0.215**	**0.289**	**0.433**	**0.289**		
Metastases						
CN	0.55 ± 0.16	0.55 ± 0.16	0.55 ± 0.16	0.60 ± 0.13	NS	0.011
PITV	1.76 ± 0.61	1.75 ± 0.61	1.76 ± 0.60	1.48 ± 0.37	NS	0.038
TC	0.932 ± 0.038	0.936 ± 0.037	0.938 ± 0.033	0.925 ± 0.053	NS	NS
HI	0.116 ± 0.044	0.119 ± 0.045	0.120 ± 0.040	0.104 ± 0.041	NS	0.016
Whole Brain						
HI	0.485 ± 0.152	0.472 ± 0.145	0.480 ± 0.145	0.322 ± 0.120	NS	< 0.001
TC	0.957 ± 0.007	0.957 ± 0.008	0.956 ± 0.008	0.959 ± 0.017	NS	NS

Abbreviations: $0.289_{2.5}$ = 0.289 pitch with 2.5 cm FW; $0.289_{1.0}$ = 0.289 pitch with 1.0 cm FW; NS = not significant.

The two-tailed *p* values were results from paired t-tests.

Table 3

Statistical Analysis of Indices for Metastases Based on Volume

	Mean and standard deviation		*p* value
	2.5 cm FW		< 2.05 cm^3 vs. ≥ 2.05 cm^3
Index	**< 2.05 cm^3**	**≥ 2.05 cm^3**	
CN	0.444 ± 0.002	0.708 ± 0.001	< 0.001
PITV	2.12 ± 0.01	1.21 ± 0.02	< 0.001
TC	0.945 ± 0.001	0.920 ± 0.007	0.03
HI	0.125 ± 0.002	0.108 ± 0.006	0.049

The two-tailed *p* values were results from paired t-tests.

Table 4

Normalized Total Dose (NTD) to Hippocampus [Gy_2] as Functions of Field Width (FW) and Pitch.

		2.5 cm FW						1.0 cm FW	
		0.215		0.289		0.433		0.289	
Patient no.	Volume (cc)	Median	Mean	Median	Mean	Median	Mean	Median	Mean
1	5.46	5.54	6.25	5.71	6.54	5.21	6.09	5.92	6.45
2	5.18	4.82	5.32	4.75	5.25	4.79	5.30		
3	4.68	5.63	6.31	5.91	6.60	5.76	6.45		
4	5.63	4.79	5.22	4.87	5.33	5.07	5.48	4.37	4.68
5	6.11	4.69	4.98	4.39	4.66	4.61	4.94		
6	5.24	4.54	4.81	4.34	4.64	4.33	4.65	4.08	4.31
7	4.19	5.76	6.09	5.11	5.54	6.63	6.52		
8	3.95	4.61	5.58	5.29	6.05	5.43	6.15		
9	5.04	8.12	9.02	8.00	8.92	7.84	8.92	8.07	8.80
10	4.46	4.50	5.10	4.55	5.11	4.33	4.95	4.15	4.66
	Mean	5.30±1.10	5.87±1.23	5.29±1.09	5.86±1.28	5.40±1.11	5.94±1.24	5.37±1.63	5.78±1.88

Table 5

Mean and Standard Deviation of Eyes and Various Treatment Plan Parameters.

	2.5 cm FW			1.0 cm FW
Parameter	**0.215**	**0.289**	**0.433**	**0.289**
Eyes (Gy_3)	3.8 ± 1.4	3.7 ± 1.2	3.8 ± 1.4	3.0 ± 1.7
MF	1.94 ± 0.33	2.10 ± 0.29	2.13 ± 0.28	2.37 ± 0.06
Gantry Period (sec)	19.0 ± 1.8	25.9 ± 2.8	38.3 ± 3.9	25.8 ± 3.6
Tx Time (min)	10.0 ± 0.9	10.2 ± 1.0	10.0 ± 1.0	21.8 ± 1.8

Abbreviations: MF = Modulation Factor, Tx = treatment